Defence Technology 36 (2024) 64–70

Contents lists available at ScienceDirect

Defence Technology

journal homepage: www.keaipublishing.com/en/journals/defence-technology

Applicability limits of the DAX test in plastic bonded explosives

Martin Künzel [a,*], Jindrich Kucera [a], Jiri Pachman [b]

[a] OZM Research, Bliznovice 32, Hrochuv Tynec 53862, Czech Republic
[b] Institute of Energetic Materials, Faculty of Chemical Technology, University of Pardubice, Studentska 95, Pardubice 53210, Czech Republic

ARTICLE INFO

Article history:
Received 29 December 2022
Received in revised form
5 September 2023
Accepted 22 September 2023
Available online 23 September 2023

Keywords:
Flyer plate
Detonation pressure
Photonic Doppler velocimetry
Semtex

ABSTRACT

The Disc Acceleration eXperiment (DAX) is one of the most recent experimental methods of performance characterization of new energetic materials. A cylindrical explosive charge accelerates a thin metallic disc and its velocity is measured continuously using photonic Doppler velocimetry. The detonation velocity is measured simultaneously. The DAX test can be used to obtain the Chapman-Jouguet (CJ) detonation pressure and to describe detonation products expansion using reduced amount of explosive. A series of DAX tests was performed at various charge diameters and disc thicknesses with Semtex 1 A plastic bonded explosive and sensitized nitromethane. The DAX-like evaluation was also applied to previously measured data of Semtex 1A and A-IX-1 explosives. The optimum disc thickness is determined by the disc to explosive mass ratio of 0.01–0.08. The repeatability of the Semtex 1 A detonation pressure results is about four times lower compared to the pressed and liquid explosives.

1. Introduction

Characterization of small quantities of energetic materials is of great interest especially in the development of new energetic materials and formulations. Various test arrangements have recently been suggested [1–3]. The Disc Acceleration experiment (DAX) is one of the most recent experimental methods of small-scale characterization of energetic materials [4–6]. It can be used to obtain the Chapman-Jouguet (CJ) detonation pressure and parameters of Jones-Wilkins-Lee (JWL) equation of state of the detonation products using reduced amount of explosive when compared to the standard scale, 25.4 mm diameter, cylinder expansion test (CYLEX). The test covers common tasks of the cylinder expansion test with reduced material consumption, a single PDV probe and no need for a precisely machined copper tube. The DAX test can also be considered a modern successor of historical small scale push plate or flyer plate tests [7,8].

In the DAX test, a thin metallic disc is accelerated by a cylindrical explosive charge and its velocity is measured using photonic Doppler velocimetry. The detonation velocity of the explosive is determined at the same time. The DAX evaluation consist of two parts: (1) the CJ detonation pressure is determined from the initial motion of the disc and (2) the energy release of the tested explosive is inferred from the whole velocity profile. Regarding the first part, the influence of the von Neumann spike (VNS), a high pressure peak of shock compression of the unreacted explosive, was assumed to be negligible in the original article [4]. Although this assumption is valid for the explosive and the flyer plates used in the original paper, its general use is questionable. For explosives with thicker reaction zones, the influence of the VNS is to be expected. In fact, the initial free surface velocities of thin plates accelerated by detonation were one of the first experimental demonstrations of the existence of the VNS [8]. It was also suggested to obtain the detonation pressure from the terminal projectile velocity and Gurney/Aziz equations [9]. Although this may provide more repeatable results compared to the original initial extrapolation, it introduces another uncertainty due to the simplifications applied. Additionally, it is sometimes difficult to obtain terminal velocities due to premature destruction of thin discs especially with highly heterogeneous explosives. Another publication [10] showed theoretical modeling of the DAX test under unfavorable conditions with voids or inert materials at the inner disc surface which may induce significant errors in the CJ pressure results.

This paper shows DAX test detonation pressure results of three different high explosives. The effects of disc thickness and

---

[*] Corresponding author.
E-mail address: kunzel@ozm.cz (M. Künzel).
Peer review under responsibility of China Ordnance Society

https://doi.org/10.1016/j.dt.2023.09.009

homogeneity of the explosive are examined and the effect of charge diameter is shown in the case of a heterogeneous plastic bonded explosive.

2. Materials and methods

2.1. Explosive charges

Three types of explosives have been studied. A liquid explosive based on amine-sensitized nitromethane (NM + EDA, 95% nitromethane+5% 1,2-diaminoethane) was used as an example of a homogeneous explosive. The density of this mixture was 1.12 g cm^{-3}. The explosive was filled in an aluminium tube (0.4 mm wall thickness) inserted in a 3 d-printed polypropylene fixture with aluminium disc glued at its end using epoxy. The length to diameter ratio of the charges was $l/d = 6$ in the NM + EDA measurements.

The results for pressed explosive charges were obtained by re-evaluation of authors' previously published data [11]. These charges were made of A-IX-1 explosive which consist of 1,3,5-trinitro-1,3,5-triazinane (RDX, 95%) desensitized with stearine/ceresine mixture (5%). The density of A-IX-1 was 1.66 g cm^{-3} and the l/d was 1.5.

Most of the experiments have been performed with a moldable plastic bonded explosive Semtex 1A (S1A). It is a well-known industrial explosive manufactured by Explosia company in Pardubice, Czechia. The explosive contains 83% of pentaerythritol tetranitrate (PETN) and 16% of non-explosive binder based on styrene-butadiene rubber plasticized with mineral oil. The explosive also contains 1% of 2,3-dimethyl-2,3-dinitrobutane as a taggant and trace amounts of stabilizers and dyes. Although exact particle size distribution of the crystalline PETN is not available, it was visible that the explosive contained a very wide range of crystal sizes of up to 1 mm. The explosive was rolled to a cylindrical shape which tightly fitted into 3 d printed confiner. The explosive was cut so that it overlapped the front surface of the fixture by 0.5 mm and the disc was clamped against it. The density of 1.45 ± 0.02 g cm^{-3} was determined from the S1A mass and fixture dimensions. In this case, the l/d was again 6.

The last data set of S1A at 36 mm diameter and $l/d = 2$ was obtained by reevaluation of the authors previously measured unpublished data from the year 2015. In these tests, the explosive was hand-packed into polypropylene tubes with 36 mm internal diameter and 2 mm wall thickness. The density of S1A in these tests was 1.42 ± 0.01 g cm^{-3} and the $l/d = 2$.

2.2. Free surface velocity measurement

The new S1A and NM + EDA experiments followed experimental set-up shown in Fig. 1. The PDV probe was supported by a holder made of 3 d-printed polylactide. The discs were made of EN AW-1050 (99.5% aluminium) plates by laser cutting and finished by tumbling to achieve diffusely reflecting surface. The thicknesses of the discs varied from 0.2 mm to 4 mm. The reevaluated data of S1A and A-IX-1 came from similarly arranged experiments just without the velocity probes and with probe holders made of foamed polystyrene.

The free-surface velocities of the discs were measured using VeloreX PDV photonic Doppler velocimeter (OZM Research). The detector signals were recorded using high-bandwidth oscilloscopes MSO64B-6-BW-4000 or DPO70404C (Tektronix). The laser beam was pointed to the target by means of a simple single-mode fiber probe terminated by a polished ceramic ferrule. The probe was fixed in a distance of 8–12 mm above the disc, perpendicular to its surface. The oscilloscope recordings were analyzed using short-time Fourier transform (STFT) with a Hamming window, time resolution of 5 ns or 10 ns and approximate velocity resolution of 30 $m\cdot s^{-1}$ or 15 $m\cdot s^{-1}$, respectively.

2.3. Detonation velocity measurement

The detonation velocity was measured using a series of 8 passive optical probes connected to the OPTIMEX-64 light analyzer (OZM Research). The instrument recorded intensities of light signals collected by the optical fibers with the time resolution of 4 ns. The distance between successive fiber probes was set to one half of the charge diameter. In the case of NM + EDA, the optical probes were just touching the thin aluminium confiner. The 3 d printed casings for the S1A charges had their inner surface covered with aluminium tape to block the light which precedes the detonation wave. The detonation velocity of the A-IX-1 charges was measured in separate experiments using axial perforated fiber optic probe [12,13].

3. Results and discussion

The DAX tests were carried out with the above described explosive samples. The initial sloped parts of the free-surface velocity profiles were extrapolated back to the explosive/aluminium interface using linear regression functions. The back-extrapolation times were estimated using shock velocity in aluminium corresponding to its initial free-surface velocity value using equation

$$t_e = b \Big/ \left(c_{Al} + s_{Al} u_{fs} / 2 \right) \tag{1}$$

In this equation, b is the disc thickness, u_{fs} is the initial value of the free surface velocity and $c_{Al} = 5.35$ $km\cdot s^{-1}$ and $s_{Al} = 1.32$ are Hugoniot constants for aluminium [14]. This method neglects the fact that the shock velocity in the disc is not constant but decreases due to the triangular shape of the input pressure pulse, leading to

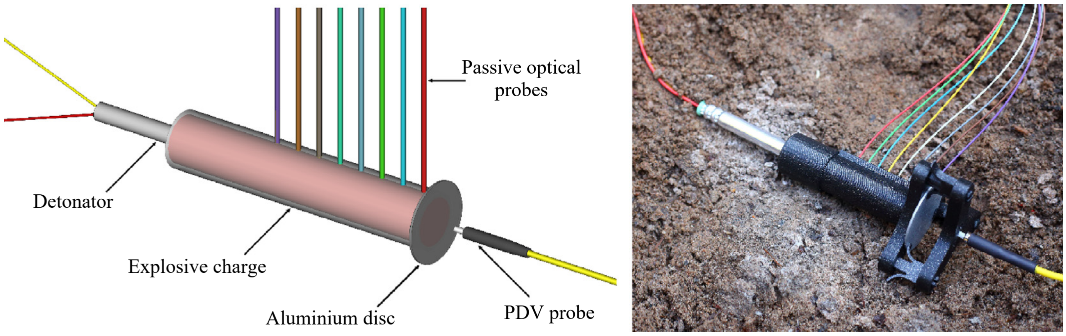

Fig. 1. Scheme and photo of the DAX test arrangement.

inherent underestimation of the extrapolated initial particle velocities. More accurate extrapolation times can be obtained when the dependence of initial velocity on disc thickness is analyzed and converted to the effective shock velocity but that may be quite inconvenient in practice due to increased complexity.

The detonation pressure was then calculated using "Method 2" described in the original paper [4]. The method uses generalized Cooper's Hugoniot curve to describe detonation products in the impedance matching procedure.

3.1. Homogeneous liquid explosive

The free surface velocity profiles measured with NM + EDA are shown in Fig. 2. In general, the profiles typically show perfect repeatability and those recorded at identical conditions overlap each other. There is no sign of the remains of the VN spike in the profiles probably because of its very short duration. There are also more than 10 clearly visible shock reverberation steps in some of the velocity profiles. It can be seen that one of the profiles (orange line) does not overlap the other two profiles after the first reverberation – in that case, pre-shot inspection of the casing found excessive amount of glue around the edge of the tube, leading to effective decrease of the charge diameter from 5 to 3 mm near the disc. This illustrates increased sensitivity of the smallest scale tests to the quality of the test setup.

3.2. Pressed explosive

The free-surface velocity profiles obtained from the experiments with A-IX-1 are quite smooth and their initial (first step) velocities decrease gradually with increasing disc thickness. As discussed in our previous publication [11], there is a significant change in slope of the profile in the first few tens of nanoseconds in the case of disc thicknesses of $\leq$1 mm which is caused by attenuating Von Neumann spike (VNS). In order to obtain the CJ detonation pressure, this first steep part was omitted in the extrapolation as can be seen in the 0.5 mm disc profile shown in Fig. 3. The velocity profiles obtained with $\leq$0.3 mm discs are apparently influenced by the VNS to an extent that makes them useless for p_{CJ} determination in this explosive.

3.3. Moldable plastic-bonded explosive

The S1A free-surface velocity profiles (Figs. 4–7) are uneven and their initial values are in some cases not even aligned in the expected order with changing disc thickness. The velocity steps are barely visible in some of the profiles and the maximum number of reverberations is four. There are also significant variations in the roundtrip times (step durations) at identical disc thicknesses. All this behavior is probably due to natural heterogeneity of the explosive, i.e. a random three dimensional field of large crystals and fine particles of PETN dispersed in the binder matrix. The detonation wave front in such a mixture is probably rough on millimeter scale. Therefore, it locally impacts the disc under other than normal angle, leading to large variations in the initial slope of the velocity profiles and corresponding extrapolated particle velocities. The non-normal shock wave impacts reportedly cause very scattered roundtrip times [15]. It was not possible to distinguish the VNS from random velocity variations so it could not have been omitted from the extrapolation – this probably led to some overestimation of the pressure in the case of thin discs.

3.4. Effect of the disc thickness

The detonation pressures evaluated using the DAX procedure vary with the disc thickness (b). There is no general trend when only the disc thickness is taken into account. This can be explained by the presence of another variables of the experimental arrangements such as the charge diameter (d) and length to diameter ratio (l/d). It was found useful to compare the experimental data sets through their disc mass (M) to explosive mass (C) ratio which is calculated using equation

$$\frac{M}{C}=\frac{b}{l}\frac{\rho_{\mathrm{Al}}}{\rho_e} \tag{2}$$

The detonation pressure values from all the experiments related to the M/C are shown in Fig. 8. The experimental points are fitted with polynomic regression curves just to see general trends. In the reevaluated data from short charges of A-IX-1 and S1A, the resulting CJ pressure decreases with increasing disc thickness (increasing M/C). The opposite trend is observed in the results from $l/d = 6$ charges of S1A and NM + EDA. This can be explained by different relative amount of energy lost due to radial expansion of the detonation products at later stages of acceleration at these different l/d ratios. For comparison, the graph contains reference values of A-IX-1 [11] and NM + EDA [16]. It can be seen that the region where the results are close to the reference values and at the same time relatively insensitive to the M/C is approximately in the range of $M/C = 0.01–0.08$.

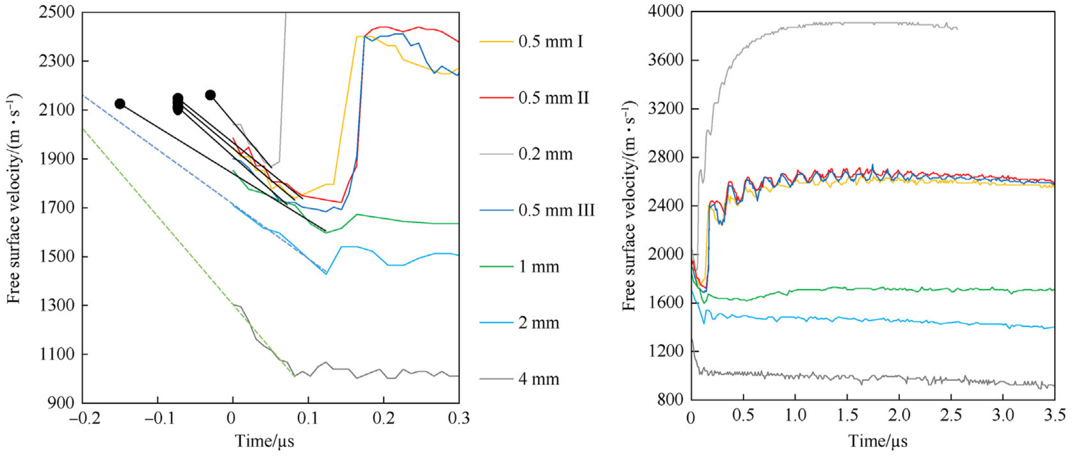

Fig. 2. Detailed view of the DAX extrapolation of the NM + EDA velocity profiles (left) and overall view (right).

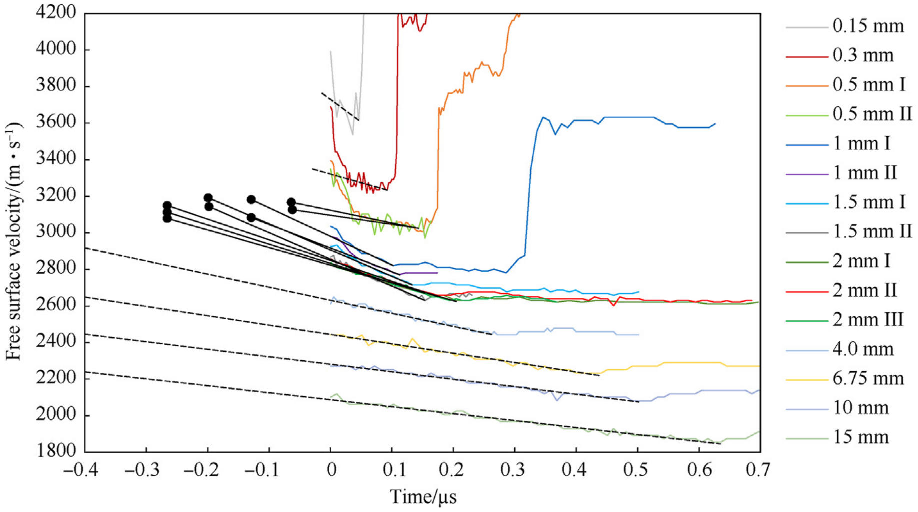

Fig. 3. Detailed views of the DAX extrapolation of the A-IX-1 profiles with different disc thicknesses.

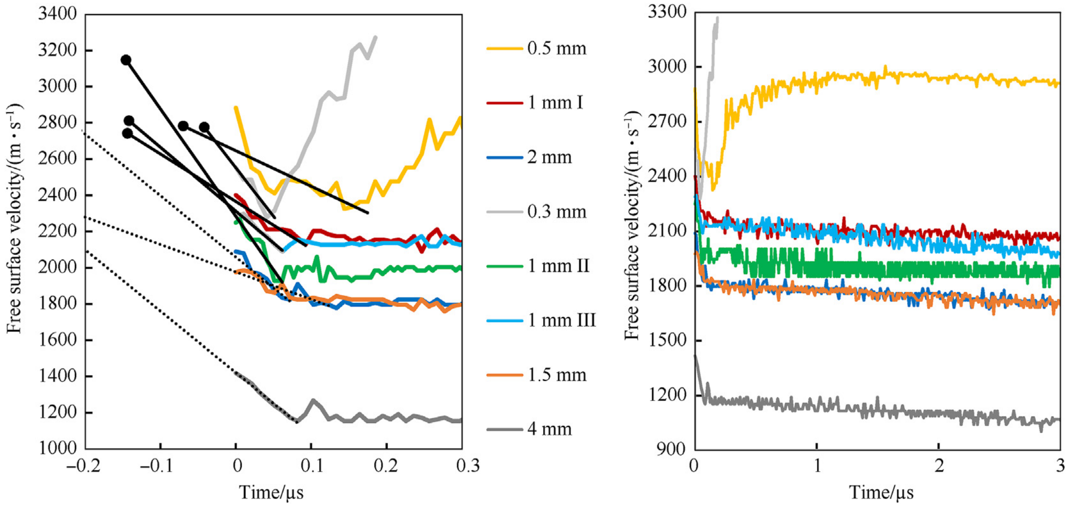

Fig. 4. Detailed views of the DAX extrapolation of the S1A velocity profiles (left) and overall view (right) for the charge diameter of 5 mm.

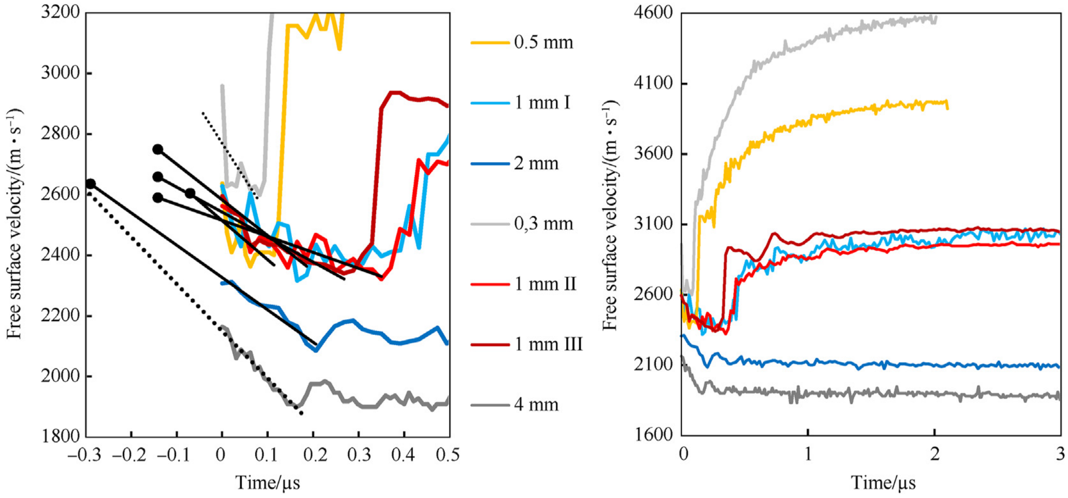

Fig. 5. Detailed views of the DAX extrapolation of the S1A velocity profiles (left) and overall view (right) for the charge diameter of 10 mm.

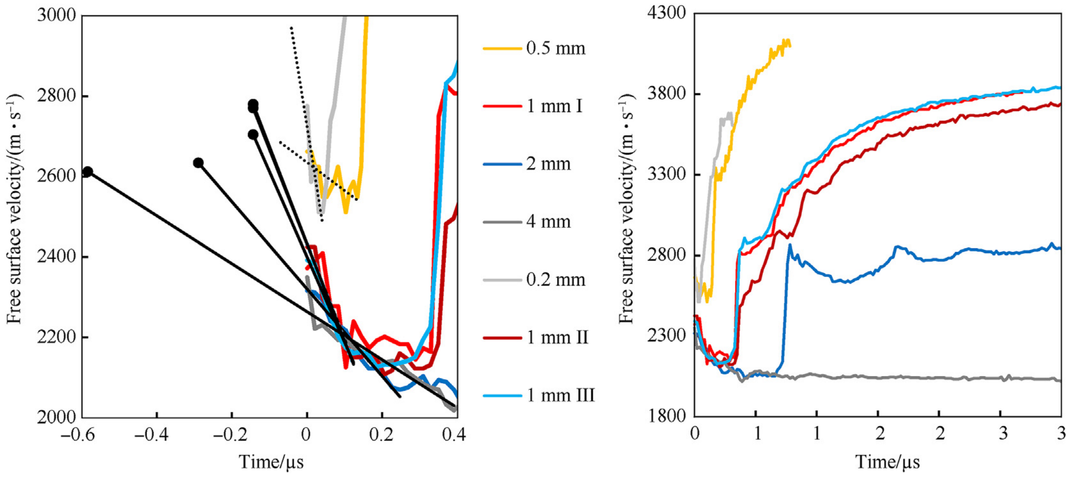

Fig. 6. Detailed views of the DAX extrapolation of the S1A velocity profiles (left) and overall view (right) for the charge diameter of 20 mm.

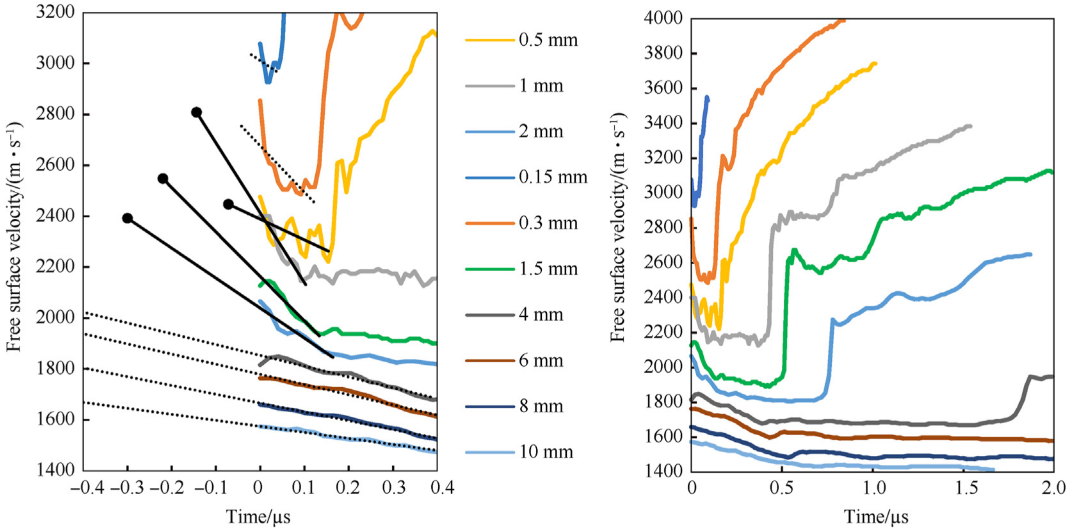

Fig. 7. Detailed views of the DAX extrapolation of the S1A velocity profiles (left) and overall view (right) for the charge diameter of 36 mm and $l/d = 2$.

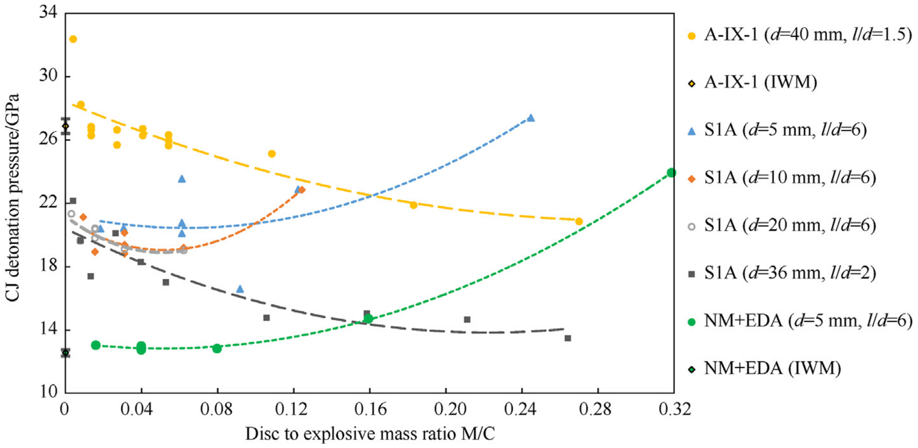

Fig. 8. The effect of the scaled disc thickness on the resulting CJ detonation pressure. The regression curves are included just to lead an eye.

The results are summarized in Table 1. The detonation velocities are shown as averages and standard deviations of all the tests at a particular charge diameter. The NM + EDA values are in agreement with the literature data [16] to within 1.6%. The detonation velocity

Table 1
Summary of the detonation parameters measured with the three explosives.

Explosive	$\rho_e/(\mathrm{g \cdot cm^{-3}})$	No. of tests	d/mm	l/d	$D/(\mathrm{m \cdot s^{-1}})$	$P_{\text{CJ-opt}}$/GPa	$P_{\text{CJ-st}}$/GPa
NM + EDA	1.12	3	5	6	6181 ± 73	12.90 ± 0.11	12.87 ± 0.10
A-IX-1[a]	1.64	9	40	1.5	8238 ± 19[b]	26.31 ± 0.40	26.59 ± 0.23
S1A	1.47	7	5	6	7254 ± 66	21.06 ± 1.27	21.48 ± 1.49
S1A	1.45	7	10	6	7350 ± 70	19.30 ± 0.47	19.45 ± 0.54
S1A	1.45	8	20	6	7398 ± 48	19.75 ± 0.76	20.20 ± 0.28
S1A	1.42	10	36	2	7340[c]	18.31 ± 1.32	n/a

[a] Re-evaluated data from previous measurements [11].
[b] The detonation velocity was measured in separate experiments [11].
[c] The detonation velocity was extrapolated from the other results and corrected for density.

of S1A at 20 mm diameter agrees with the available literature values [17,18] and authors' previous measurements [19] to within 1%. At lower charge diameters, the detonation velocity slightly decreases as it is expected due to the diameter effect.

The detonation pressures marked $P_{\text{CJ-opt}}$ in Table 1 are averaged from the tests with the disc thicknesses corresponding to $M/C = 0.01–0.08$ while the $P_{\text{CJ-st}}$ are averaged from repeated experiments with the same disc thickness (1 mm for S1A and 0.5 mm for A-IX-1 and NM + EDA). The measured NM + EDA detonation pressure is at least 3% higher than the recent literature values of 12.5–12.6 GPa [16,20] obtained using the impedance window method (IWM). This is most probably due to the significant impedance mismatch between the NM + EDA and aluminium which causes initial VNS high pressure shock reflection back to the approaching reaction zone of the explosive. The A-IX-1 detonation pressure is consistent with authors' previous results obtained using the flyer plate and impedance window methods [11]. The standard deviation of the detonation pressure values obtained with different disc thicknesses correspond to 1.5% uncertainty in the case of A-IX-1.

For the S1A, there is only one available experimental detonation pressure value of 17 GPa [18] which is more than 15% below the current result. The reason for such a high difference remains unclear. The CJ pressures obtained at 5 mm charge diameter seem to be unrealistically high despite slightly higher density in these tests. The standard deviations are 6.0%, 2.4% and 3.8% for charge diameters of 5 mm, 10 mm and 20 mm, respectively, when all the discs within the M/C range from 0.01 to 0.08 are considered. The reevaluated data of 36 mm diameter S1A tests show standard deviation of 7.2% probably due to suboptimal build quality of the test setups coupled with their small length to diameter ratio. When only the repeated experiments with a single disc thickness are considered, the standard deviations of the A-IX-1 and 20 mm S1A tests drop but they remain about the same in the case of 5 mm and 10 mm S1A tests.

4. Conclusions

(1) Measurement of the CJ detonation pressure using DAX test is reproducible to within 0.8% in liquid homogeneous explosives (NM + EDA). The free surface velocity profiles from repeated experiments overlap each other.
(2) In the solid pressed explosive (A-IX-1), the CJ detonation pressure reproducibility is within 1.5%.
(3) In the plastic bonded explosive with a wide particle size distribution (Semtex 1 A), the reproducibility is reduced to 2%–7%. The initial parts of the free-surface velocity profiles are significantly scattered in contrast with those obtained with the pressed or liquid explosives.
(4) The thickness of the disc used for the test must be as small as possible to reduce the errors from extrapolation but large enough to attenuate the initial Von Neumann spike. For the explosives tested in this study, the optimum disc thickness where linear extrapolation of the velocity profile seems to be sufficient corresponds to the disc to explosive mass ratio of 0.01–0.08.
(5) At small charge diameters (5 mm), the scatter in the DAX test results of heterogeneous high explosives can be large enough to hide the expected diameter effects, making the test useless. On the contrary, small diameter charges of homogeneous explosives may still provide correct and repeatable results.

Declaration of competing interest

The authors declare that they have no known competing financial interests or personal relationships that could have appeared to influence the work reported in this paper.

References

[1] Cutting JL, Chau HH, Hodgin RL, Hoffman DM, Garcia F, Lee RS, et al. A small-scale screening test for HE performance: application to the new explosive LLM-105. In: 11th international detonation symposium; 1998. p. 828–35.
[2] Biss MM. Removing full-scale testing barriers: energetic material detonation characterization at the laboratory scale. ARMY RESEARCH LAB ABERDEEN PROVING GROUND MD WEAPONS AND MATERIALS RESEARCH DIR/WEAPONS MATERIALS DIV.; 2012.
[3] Rumchik C, Nep R, Butler GC, Breaux B, Lindsay C. The miniaturization and reproducibility of the cylinder expansion test. In: AIP conference proceedings, vol. 1426. American Institute of Physics; 2012. p. 450–3. 1.
[4] Lorenz KT, Lee EL, Chambers R. A simple and rapid evaluation of explosive performance. Propellants, Explos Pyrotech 2015;40(1):95–108.
[5] Maines WR, Kittell DE, Hobbs ML. Combined mini-cylex & disk acceleration tests in type K copper, propellants explos. Pyrotech 2018;43(5):506–11.
[6] DeHope A, Zhang M, Lorenz KT, Lee E, Parrish D, Pagoria PF. Synthesis and small-scale performance characterization of new insensitive energetic compounds (No. LLNL-CONF-669680). Livermore, USA: Lawrence Livermore National Lab. (LLNL); 2015.
[7] Kury JW, Dorough GD, Sharples RE. Energy release from chemical systems. USA, Princeton: Third Symposium on Detonation; 1960. p. 738–51.
[8] Duff RE, Houston E. Measurement of the Chapman–Jouguet pressure and reaction zone length in a detonating high explosive. J Chem Phys 1955;23(7):1268–73.
[9] Chaos M, Lee EL, Lorenz KT. Experimental determination of chapman-jouguet pressure using disc acceleration eXperiment (DAX) data, report No. LLNL-CONF-753452. Livermore, USA: Lawrence Livermore National Lab. (LLNL); 2018.
[10] Sutherland G, Sable P, Borg J. Simulations of disk acceleration experiments. In: AIP conference proceedings, vol. 1979. AIP Publishing LLC; 2018. p. 100040. 1.
[11] Pachman J, Künzel M, Němec O, Majzlík J. A comparison of methods for detonation pressure measurement. Shock Waves 2018;28(2):217–25.
[12] Prinse WC, van Esveld R, Oostdam R, van Rooijen M, Bouma R. Fiber optic techniques for measuring various properties of shock waves. In: 23rd international congress on high-speed photography and photonics, Moscow, Russia, vol. 3516; 1999. p. 246–51.
[13] Künzel M, Matyáš R, Vodochodský O, Pachman J. Explosive properties of melt cast erythritol tetranitrate (ETN). Cent Eur J Energ Mater 2017;14(2).
[14] Choudhuri D, Gupta YM. Shock compression and unloading response of 1050 aluminum to 70 GPA. AIP Conference Proceedings, American Institute of Physics 2012;1426(1):755–8.
[15] Bukovsky EV, Chambers RD, Lee EL, Lorenz KT. The shell acceleration experiment (SAX)-A modern corner-turning experiment, report No. LLNL-PROC-

754038. Livermore, USA: Lawrence Livermore National Lab. (LLNL); 2018.

[16] Utkin AV, Mochalova VM, Logvinenko AA. Effect of diethylenetriamine on the structure of detonation waves in nitromethane. Combust Explos Shock Waves 2013;49(4):478–83.

[17] Elbeih A, Pachman J, Trzciński WA, Zeman S, Akštein Z, Šelešovský J. Study of plastic explosives based on attractive cyclic nitramines Part I. Detonation characteristics of explosives with PIB binder. Propellants, Explos Pyrotech 2011;36(5):433–8.

[18] Majzlík J, Dusík V. DETPAR-The cataloque of detonation parameters. Pardubice: University of Pardubice; 2002.

[19] Künzel M, Němec O, Pachman J. Optimization of wall velocity measurements using photonic Doppler velocimetry (PDV). Cent Eur J Energ Mater 2015;12(1):89–97.

[20] Bouyer V, Sheffield SA, Dattelbaum DM, Gustavsen RL, Stahl DB, Doucet M, et al. Experimental measurements of the chemical reaction zone of detonating liquid explosives. In: AIP conference proceedings, vol. 1195. American Institute of Physics; 2009. p. 177–80. 1.